Particulate inorganic carbon quotas by coccolithophores in low oxygen/low pH waters off the Southeast Pacific margin

Francisco Díaz-Rosas[1,2], Cristian A. Vargas[2,3], and Peter von Dassow[1,2]

[1]Facultad de Ciencias Biológicas, Departamento de Ecología, Pontificia Universidad Católica de Chile, Santiago, Chile
[2]Millennium Institute of Oceanography (IMO), Universidad de Concepcion, Concepcion, Chile
[3]Coastal Ecosystems & Global Environmental Change Lab (ECCALab), Department of Aquatic Systems, Faculty of Environmental Sciences, Universidad de Concepción, Concepcion, Chile

Correspondence to: Francisco Díaz-Rosas (fdiazrosas7@gmail.com)

Abstract. A predicted consequence of ocean acidification is its negative effect on the pools of Particulate Inorganic Carbon (PIC) that are essential for 'ballasting' the sinking of organic carbon, potentially leading to decreased subsurface oxygen. To explore such possible feedbacks, we investigated the relationships between PIC, coccolithophores, carbonate chemistry, and dissolved oxygen in the Southeast Pacific open ocean oxygen minimum zone, which naturally exhibits extremely low dissolved oxygen, low pH, and high pCO$_2$ levels. Measurements of PIC and coccolithophore counts during late-spring 2015 and mid-summer 2018 revealed that coccolithophores, particularly *Gephyrocapsa (Emiliania) huxleyi*, significantly contributed to PIC through the shedding of coccoliths in the upper waters. On average, about a half of the PIC was attributed to countable coccoliths, with significantly diminished quotas observed below the euphotic depth. Temperature, oxygen, and pH were identified as key variables influencing PIC variation. PIC quotas were similar to those reported in other upwelling zones. However, PIC:POC ratios were substantially lower than what has been reported both in other open ocean and coastal margin areas, an effect that was more pronounced within the vertically defined oxygen minimum zone core. This study contributes to understanding the role of coccolithophores in PIC pools and suggests that the presence of low O$_2$/low pH subsurface waters does not inhibit coccolithophore PIC quotas but may decrease the role of PIC in ballasting the export of organic carbon.

1 Introduction

The Particulate Inorganic Carbon (PIC) pool, a significant component influencing marine C cycles and atmospheric reservoirs (Ridgwell and Zeebe, 2005), originates from various sources, including land transport to coastal margins (Cai, 2011) and biological processes such as phytoplankton calcification (Taylor and Brownlee, 2016). Coccolithophores, particularly the cosmopolitan species *Gephyrocapsa (Emiliania) huxleyi*, significantly contributes to PIC through coccolith production, impacting C sequestration and nutrient cycling in the global pelagic ocean (Monteiro et al., 2016; Balch, 2018). In turn, changes in PIC dynamics driven by alterations in coccolithophore community at different spatial and temporal scales feedback into the ocean-atmosphere system (Balch et al., 2016; Claxton et al., 2022). For example, ocean acidification (OA or decreased pH and

carbonate ion concentration) can impair coccolithophore calcification (Riebesell et al., 2000; Barcelos e Ramos et al., 2010; von Dassow et al., 2018; Kottmeier et al., 2022; von Dassow, 2022), which could lead to diminished $CaCO_3$ fluxes to the seafloor, favouring the respiration of more organic material and potentially decreasing both organic C flux and mid-water O_2

35 levels (Hofmann and Schellnhuber, 2009; Zhang et al., 2023). In this context, the relationships between coccolithophore PIC quotas with pH/pCO$_2$ and O_2 in natural oxygen minimum zones (OMZs), where pH and O_2 levels can become extremely low, are of particular interest.

While the Atlantic Ocean and the Atlantic sector of the Southern Ocean have been more extensively sampled for PIC, the Pacific Ocean remains underrepresented in PIC and coccolithophore data, although information is accumulating on

40 coccolithophore distributions in the Indian Ocean, the subpolar Pacific, and the Southern Ocean (Balch et al., 2018; Oliver et al., 2023). Early satellite imagery showed relatively lower PIC levels in extensive upper Pacific waters compared to the Atlantic (Brown and Yoder, 1994). However, higher subsurface PIC concentrations, at depths greater than the detection limit of satellites, have been associated with coccolithophore blooms in remote Southeast Pacific waters (Beaufort et al., 2008; Oliver et al., 2023). The Great Calcite Belt, a remarkable basin-scale coccolithophore feature in the Southern Ocean, is primarily

45 sustained by the growth of *G. huxleyi* (Balch et al., 2016; Balch and Mitchell, 2023) and has attracted particular attention, as it progresses southward every year with peaks in the austral summer (Hopkins et al., 2019). Temperature, competition with diatoms for nutrients, and Fe availability have been proposed as factors controlling coccolithophore distributions in the Southern Ocean (Oliver et al., 2023 and references therein).

Vast OMZs are a persistent feature of the tropical and subtropical Eastern Pacific (Schmidtko et al., 2017), and it is known

50 that these zones tend to have low pH and high pCO$_2$ levels (Torres et al., 2002, 2011; Beaufort et al., 2011; Vargas et al., 2017; Vargas et al. 2021). Although the pH and pCO$_2$ levels in these waters can inhibit coccolithophore growth and calcification in laboratory settings, field observations suggest more complex relationships (Beaufort et al., 2011; Müller et al., 2015; von Dassow et al., 2018). Nevertheless, there is still very limited data on how PIC, POC, pH, and O_2 might interact in OMZ systems. Here, we present measurements of PIC alongside counts of coccolithophores and estimates of PIC derived from them,

55 collected during sampling in spring 2015 and summer 2018 off the Southeast Pacific margin (~ 20-35º S). We estimate the proportion of total PIC accounted for by coccospheres and detached coccoliths pools and examine how these coccolithophore-PIC quotas correlate with various physical and chemical parameters, with a particular focus on the effects of low pH/high pCO$_2$ conditions associated with O_2-deficient waters. Additionally, we discuss other in-situ variables recognized as factors influencing coccolithophore growth. Finally, we compare the PIC concentrations in the Southeast Pacific with those reported

60 in other oceanic regions.

2. Materials and Methods

2.1 Sampling

The sampling consisted of two cruises conducted in waters off the Southeast Pacific margin, north-central of Chile (Fig. 1a).
In spring 2015 (LowpHOX 1), we vertically screened six stations along an inshore-offshore transect off Iquique (~20º S; sts.
65 T1-T6), along with six stations arranged latitudinally between 22º S and 29.5º S (sts. L1-L6). During summer 2018 (LowpHOX
2), three of the inshore-offshore stations were replicated (sts. T1, T3, T5), along with seven stations sampled southward down
to ~34º S (sts. Lander and Hydro; Fig. 1a). In depth, the sampling crossed both the euphotic zone and OMZ core (Fig. 1b, 2c-
e, k-n). The predominant oceanographic conditions during these two cruises, as reported and discussed by Vargas et al., (2021),
provide the context for the new data presented here.

70 At each station, discrete seawater samples were collected, filtered, stored, and moved to the lab for the determination of PIC
(section 2.2) and coccolithophore standing stocks (section 2.3). Due to seawater availability onboard in 2018, sampling for
coccolithophores only reached 100 m, except for station T5, which reached a depth of 2000 m. This contrasts with 2015
sampling reaching equal or greater 350 m depths (max. 1000 m in T3 and T4). Complete PIC measurements and
coccolithophore abundances are provided in the Supplement (Tables S1-S2). As ancillary data, 1-m averaged SST, SSS,
75 oxygen, and fluorescence continuous profiles, as well as, discrete profiles of Chl-a, nutrients, Particulate Organic Carbon
(POC), and carbonate system were included (see methods in Vargas et al., 2021). These physical and chemical data were
extracted from Vargas et al. (2023a, b, c). The euphotic depth (Z_{eu}) was estimated by calculating the depth at which the
Photosynthetically Active Radiation (PAR) is reduced to 1 % of surface levels, using the attenuation coefficients (K_d490)
provided by the Bio-Geo-Chemical products based on the Copernicus-GlobColour processor. The averaged Kd(490) values (3
80 x 3 pixels and 3-day average) were converted into K_d(PAR) values following the model of Morel et al. (2007), and the 4.6
optical depth calculated as ln(100)/K_d(PAR) (Morel, 1988). Where available, a good fit was found between the euphotic zone
depth derived from satellite observations and PAR obtained from a sensor attached to the CTD (Fig. S1). Lastly, the OMZ
core was defined to be within the thresholds of 5 % of the maximum O_2 concentration at each station occurring between 0 and
34 m depth.

85 ### 2.2 Particulate inorganic carbon standing stocks

For the measurements of PIC (hereinafter referred to as PIC_{Total}), we followed a slightly modified version of the procedure
introduced by Poulton et al. (2006). In summary, we filtered between 0.1-1.5 L of seawater (increasing with sampled depth)
onto 25 mm polycarbonate filters with a 0.4 μm pore size. The filters were immediately rinsed with a squirt of potassium
tetraborate solution (to maintain pH > 8.0 while in storage) and stored in metal-free Falcon tubes at -20º C until transit to the
90 lab. Subsequently, Ca^{2+} was extracted with nitric acid and quantified using Inductively Coupled Plasma Atomic Mass
Spectrophotometry facilities at the Bigelow Laboratory for Ocean Sciences. A correction was made to correct for potential
excess of Ca^{2+} due to Na^+ residues that might be left on the filters. The PIC calculations were expressed in mmol C m^{-3}. We

examined the association between calcification (PIC) and POC (from Vargas et al., 2021) using PIC:POC ratios. Moreover, PIC:POC ratios were built (both PIC$_{Cocco}$ and PIC$_{Total}$ values recorded in 2015 and 2018 are mostly equivalent building

95 PIC:POC ratios, except for a large mismatch at the 2015 station L4, see Fig. S2), and binned above, within, and below the OMZ core, to assess the influence of this OMZ on PIC and POC concentrations. These ratios were plotted against those reported for other open ocean or coastal margins (see Balch et al., 2018). To that, PIC and POC data was obtained from the SEABASS (Werdell et al., 2003) and BCO-DMO repositories (Balch, 2010), and PIC:POC ratios binned at surface (< 5 m depth), sub-surface (5-100 m), and below surface layers (100-500 m).

100
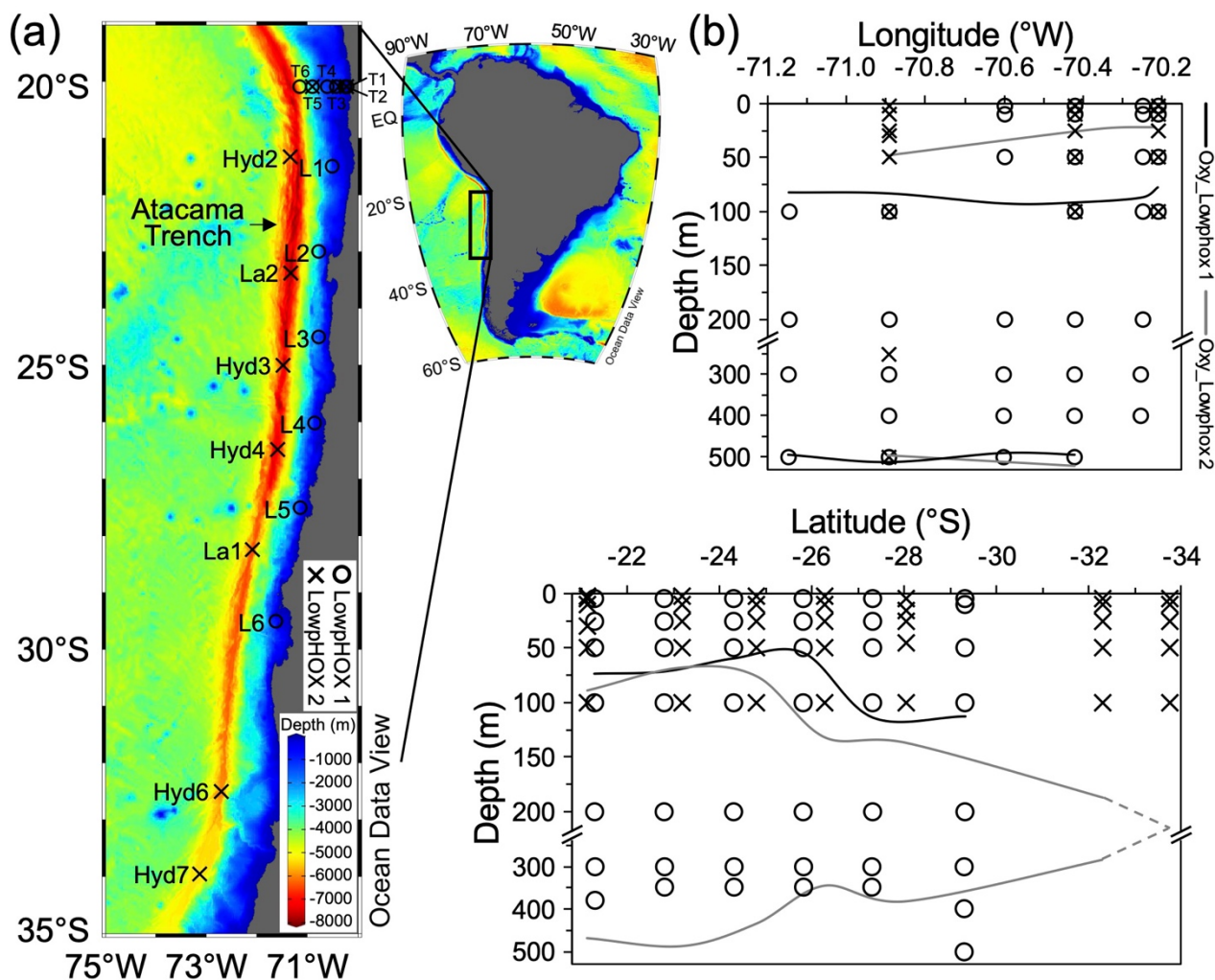
Figure 1: (a) Map of the Southeast Pacific margin showing the study site and stations sampled during late-spring 2015 (circles) and mid-summer 2018 (crosses). (b) Sampling depth coverage for coccolithophores, highlighting areas crossing the OMZ core (black and grey lines), defined as the depths within 5 % of the maximum O₂ concentration at each station. Note the OMZ core at stations T1-

105 **T2 and in the 2015 latitudinal section extends to the seafloor. 'Oxy' indicates the oxycline. Map produced by Ocean Data View (Schlitzer, 2024), with bathymetry based on the GEBCO chart (GEBCO, 2023).**

2.3 Coccospheres and detached coccoliths standing stocks

For enumeration of coccospheres and detached coccoliths, between 0.1 to 1.0 L of seawater (increasing with depth) were filtered onto 25 mm polycarbonate filters with a 0.8 μm pore size, left to dry at room temperature in Petri dishes, and stored
110 with desiccant until microscopy analyses. The counts of total coccospheres were made as described in Díaz-Rosas et al. (2021), through cross-polarized light microscopy (Zeiss, Axioscope 5) covering 5.1 mm^2 of the filter area corresponding to a range of 1.9-16.3 mL of seawater analysed. For counts of total detached coccoliths, eleven fields of view per filter were screened (224 x 165 μm per frame) at 630x magnification (oil immersion objective), covering 0.41 mm^2 of the filter area, corresponding to total volumes of 0.2-1.3 mL of seawater analysed. An issue arose where the filters from inshore-offshore 2015 sampling (20º
115 S; Stations T1-T6) exhibited excessive brightness under cross-polarized light microscopy, for which counts were made through scanning electron microscopy (SEM) analysis (Quanta FEG 250). For the quantification of coccosphere abundances (see equation in Díaz-Rosas et al., 2021), between 28-48 images taken at 800-1500x magnification were examined per filter, covering from 5 to 6 mm^2 of the filter area corresponding to a range of 2.1-18.4 mL of seawater analyzed. For total detached coccolith abundances, between 4-5 images were examined per filter, covering from 0.6 to 1.0 mm^2 of the filter area
120 corresponding to a range of 0.2-2.8 mL of seawater analyzed. Layers of coccoliths detached from *G. huxleyi* (Fig. S3a-d) were added to the detached-coccolith counts. Collapsed coccospheres were included when they remained mostly intact, but when more disintegrated could not be accurately counted, especially as they were often less reflective than intact coccospheres and coccoliths (Fig. S3e-h). In a subset of samples, collapsed coccospheres were estimated to contribute < 21 % (min. = 0 %, average = 7.1 %) of the total number of coccospheres. To check for differences between counts obtained through cross-
125 polarized light microscopy and SEM examination, five samples with varying coccolithophore abundances were analyzed with SEM as outlined above, revealing a good fit between coccosphere and coccolith abundances from both methods (Fig. S4), allowing for comparison.

2.4 Diversity of coccospheres and detached coccoliths

SEM was used for samples from T1 to T6 and L1 (at 5 and 25 m), L2 (at 5 and 50 m) and L3 (at 5 m) in 2015, classifying
130 coccospheres and detached coccoliths according to Young et al. (2003). Between 6 to 11 and 4 to 5 images per filter, depending on magnification, were examined for coccospheres and coccoliths classification, respectively. To estimate the absolute abundances of coccospheres and coccoliths at the species or genus level, the relative abundance of each species or genus was multiplied by the total coccospheres and coccoliths abundances. Due to limited resolution, it was not always possible to differentiate between *G. parvula* and *G. ericsonii* coccospheres, so they were merged into the *G. parvula/ericsonii* category,
135 which is phylogenetically supported (Bendif et al., 2016, 2019). Moreover, as some of the small coccoliths detached from *G. parvula/ericsonii* might be overlooked (2.0 µm in length), the few coccoliths found in distal-shield view, and the coccoliths from *G. huxleyi* (3.6 µm in length) were merged into the *Gephyrocapsa* < 4 μm category. Larger coccoliths (> 5 µm in length) were classified into species or genus, being subtracted from total counts of coccoliths obtained in the same SEM image (see

above) to obtain the number of coccoliths < 4 µm. Most rare detached coccoliths were grouped in the miscellaneous category

140   that include *Syracosphaera* spp., *Acanthoica* spp., *Discosphaera tubifera*, *Umbellosphaera* spp., and *Umbiliscosphaera* spp. Moreover, the counts of detached coccoliths from *Calcidiscus leptoporus* might contain a few coccoliths of *Oolithotus* spp. as it was not always possible to differentiate them. In all surface samples taken in 2018, as well as in samples L4 to L6 from 2015, species dominating the coccosphere and coccolith pools were identified using cross-polarized light microscopy (63x objective, Zeiss Axioscope 5) following Frada et al. (2010).

145   2.5 Coccolithophore specific PIC quotas

The taxonomic classification of coccospheres and coccoliths was used to estimate the specific PIC quotas of coccospheres + coccoliths (hereinafter referred to as PIC_{Cocco}) by employing conversion factors according to Young and Ziveri (2000). To obtain the coccolith mass (in pg $CaCO_3$), the cube of the mean distal-shield length of coccoliths (= biovolume in μm^3) measured in the SEM images (see Table S3) was multiplied by the respective shape factor (K_s taken from Young and Ziveri (2000), and

150   by the density of calcite (2.7 g cm^{-3}). Then, the absolute abundances of coccospheres and detached coccoliths were multiplied by the coccolith mass, and the PIC_{Cocco} stocks expressed in mmol C m^{-3}. Before the conversion, the number of coccospheres was converted to coccoliths by using the compilation of coccoliths per coccosphere in Yang and Wei (2003). For *G. huxleyi*, the 17 coccoliths per coccosphere determined by Beaufort et al. (2011) in the study site was applied in agreement with those seen in SEM images. We did not account for variation in coccoliths per coccosphere or in mass content per coccolith among

155   *G. huxleyi* morphotypes. The PIC_{Cocco} is then given by the sum of coccolith mass composed by coccospheres and detached coccoliths. This procedure was then applied to all the samples, using the *G. huxleyi* PIC quota (mass = 2.5 pg $CaCO_3$ per coccolith; see Table S3) as a maximum threshold, a situation observed during blooms (see below).

3 Results

3.1 Oceanographic conditions. Standing stocks of coccolithophores, PIC, POC, and PIC:POC ratios

160   Surface (mixed) layer temperatures exceeded 21 °C to the north and offshore, while surface temperatures were below 17 °C near the coast, in the north and south of 21° and 24º S latitude in 2015, and south of 29º S in 2018 (Fig. 2a). The pycnocline (Fig. 2b) and oxycline (Fig. 2c) roughly paralleled the thermocline in both years. In 2015, the oxycline was always in the upper 50 m. In 2018, the depth of the oxycline increased to between 50 and 75 m south of 26° S. The estimated Z_{eu} was often near the base of the oxycline (Fig. 2c). At all stations, the oxycline and Z_{eu} were always shallower than 100 m. In these well-

165   illuminated waters, peaks of phytoplankton were observed in both 2015 and 2018 (Fig. 2d-e).

Nitrate and phosphate levels were low above the pycnocline (< 10 and < 1 µM, respectively), and increased below (to approximately 20 µM and 2 µM respectively; Fig. 2f-g). Both pH and Ω calcite declined sharply while pCO_2 increased with depth through the oxycline (Fig. 2h-j). Increased nitrate coincided with higher pCO_2 and lower pH (Fig. S7). In this upwelling zone, high nitrate levels are associated with lower pH (Fig. S7b). At depth, decomposition depletes oxygen while releasing

170 nitrates and CO_2, and as nitrate-rich waters rise to the surface, they bring low oxygen/low pH and high pCO$_2$ with them (Fig. S7c-d). The more nitrate present, the more oxygen has likely been consumed in deep waters before upwelling. As interchange with the atmosphere and photosynthesis occurs, oxygen levels rise, pCO$_2$ decreases, pH increases, and calcite stability increases (higher Ω calcite; Fig. S7d-f). Additionally, high pCO$_2$ concentrations result in low pH and Ω calcite in these waters (Fig. S7g-i).
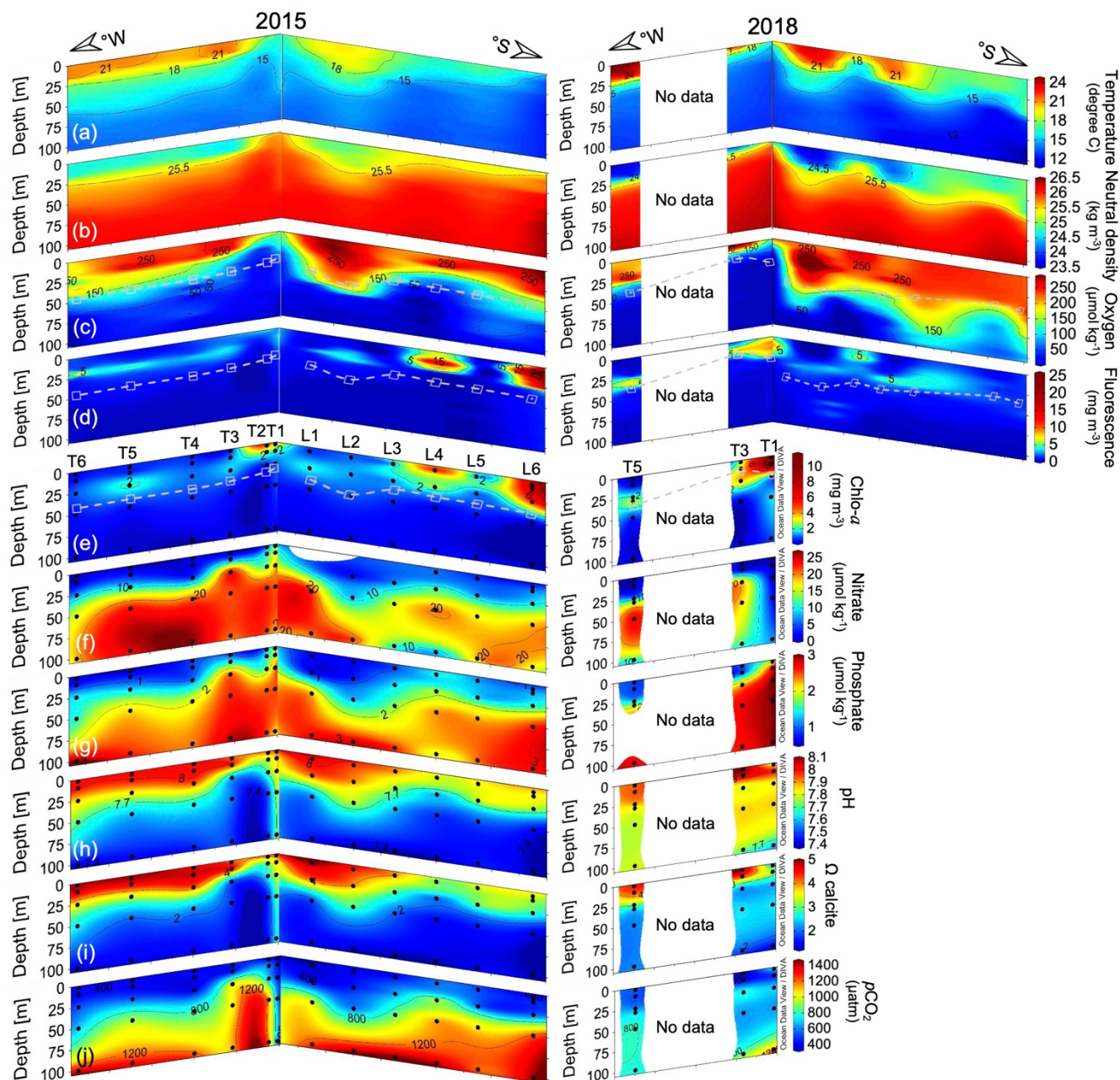
Figure 2. Spatial variation in physical–chemical–biological parameters along with PIC$_{Total}$ and coccolithophore standing stocks and their contribution to PIC (PIC$_{Cocco}$) recorded during late-spring 2015 (left) and mid-summer 2018 (right). Temperature (a), neutral density (b), oxygen (c), fluorescence (d), Chl-*a* (e), nitrate (f), phosphate (g), pH (h), Ω calcite (i), *p*CO$_2$ (j), PIC$_{Total}$ (k), coccospheres (l), detached-coccoliths (m), and PIC$_{Cocco}$ sections (n) versus long-lat and depth with sample locations (solid black circles). Continuous profiles shown in (a-d) are 1-m binned. Dashed grey lines indicate the euphotic depth in plots c-e and k-n. PIC = Particulate Inorganic Carbon. All-depth profiles of variables in plots e and k-n are provided in Supplementary Figures S5-S6.
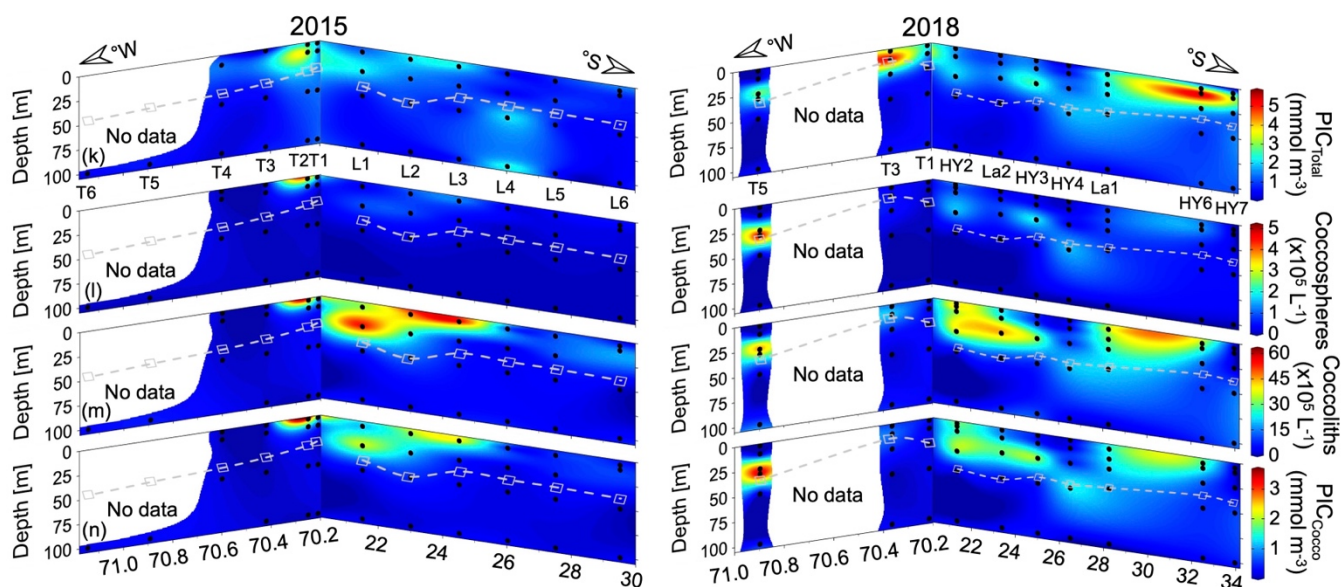
Figure 2. continuation.

In late-spring 2015, the highest abundances of coccospheres (> 3.0 x10^5 L^{-1}) and detached coccoliths (> 45 x10^5 L^{-1}), along

185   with PIC$_{Total}$ (> 3 mmol m^{-3}) and PIC$_{Cocco}$ quotas (> 2 mmol m^{-3}), were found in surface or near-surface waters (< 25 m depth) closer to the coast at ~20º S (stations T1-T2), extending south to ~24º S (stations L1-L3; Fig. 2k-n). Two years later, in mid-summer 2018, the highest surface stocks of coccolithophores (5.2 x10^5 coccospheres L^{-1}), PIC$_{Total}$ (5.3 mmol m^{-3}), and PIC$_{Cocco}$ (3.7 mmol m^{-3}) were found at ~20º S (stations T3 and T5), as well as southward between ~22-25º S and ~28-33° S (Fig. 2k-n). Throughout the station depths, PIC$_{Total}$ ranged from 0.18 to 3.81 mmol m^{-3} in 2015 and from 0.08 to 5.86 mmol m^{-3} in 2018

190   (Fig. 2k). Coccosphere abundances reached maxima of 3.9 x10^5 and 5.2 x10^5 L^{-1}, and abundances of detached coccoliths reached maxima of 63 x10^5 and 49 x10^5 L^{-1} in spring 2015 and summer 2018, respectively (Fig. 2l-m). Over these abundance ranges, coccospheres and detached coccoliths varied in direct proportion (Fig. S8). In surface waters (0-30 m), the ratio of coccoliths to coccospheres in 2015 averaged 39 (range: 4-104; n = 20) and 40 in 2018 (range: 6-287; n = 32). The estimated PIC quotas produced by coccolithophores ranged from 0.02 to 3.60 mmol m^{-3} in 2015 and from 0.01 to 3.69 mmol m^{-3} in 2018

195   (Fig. 2n). Coccosphere and coccolith abundances, as well as PIC quotas, diminished substantially below 50 m depth (~ Z$_{eu}$) (see Fig. S5-S6).

Across all samples, POC ranged from 22.7 to 250.0 mmol m^{-3} in 2015 and from 26.1 to 501.6 mmol m^{-3} in 2018. As expected from two biologically-driven carbon sources, POC correlated closely with Chl-a (Fig. S9a), and the two-orders-lower PIC$_{Total}$ varied significantly with POC (Fig. S9b). Surface PIC:POC ratios ranged from 0.002 to 0.030 in 2015 (mean = 0.011, n = 18)

200   and from 0.001 to 0.014 in 2018 (mean = 0.007, n = 10).

3.2 Diversity of coccospheres and detached coccoliths

In 2015 and 2018, *G. huxleyi* was the numerically dominant coccolithophore south of 20° S (Fig. S10-S11). It co-dominated with *G. parvula/ericsonii* in all 2015 samples at 20° S, where there was no consistent variation in the relative abundance of these taxa (Fig. 3). The relative abundance of larger taxa increased below the Z_{eu}, reaching 0-18 % and 0-15 %, respectively
205 (Fig. 3), as total coccosphere and coccolith abundances declined sharply.

3.3 Distribution of coccolithophore-PIC quotas

After converting the coccospheres and coccoliths densities recorded at ~20º S in 2015 to coccolith-PIC values allometrically, we observed that the majority of the coccolithophore PIC mass (> 2 mmol m^{-3}) was produced near the coastline in waters shallower than 30 m. Below the Z_{eu}, the sharp decline in the numerical abundances of coccospheres (< 0.1 x10^5 L^{-1}) and
210 detached coccoliths (< 10 x10^5 L^{-1}) decreased coccolithophore PIC pools to below 1 mmol m^{-3}.
Above the Z_{eu}, the coccospheres and detached coccoliths of *G. huxleyi* and *G. ericsonii/parvula* dominated the PIC quotas (Fig. 4a). In contrast, detached coccoliths of numerically rarer taxa, such as *C. leptoporus*, *Helicosphaera* spp., and *G. oceanica*, contributed significantly to PIC quotas below the Z_{eu}, often exceeding the contributions of the smaller *Gephyrocapsa* species at most stations (Fig. 4b-c).
215 A significant positive linear relationship was found between the PIC$_{Total}$ and PIC$_{Cocco}$ values both in the upper 100 m and across all sampled depths (Fig. 5a-b). In all but three cases, the calculated PIC$_{Cocco}$ values were lower than the measured PIC$_{Total}$. These exceptions corresponded to a high total numerical abundance of *G. huxleyi*. Another notable exception was station L1 at 25 m, where *C. leptoporus* and *Helicosphaera* spp. contributed 51 % and 20 % of the coccosphere PIC (2.23 mmol m^{-3}), and the estimated total PIC$_{Cocco}$ (5.1 mmol m^{-3}) was about twice the measured PIC$_{Total}$. In the upper 100 m, PIC$_{Cocco}$ quotas were
220 primarily comprised of detached coccoliths (67 % of the accounted PIC$_{Total}$), with a roughly similar contribution from coccospheres throughout the sampled depths (Fig. 5c). On average, coccoliths were estimated to account for 48 % of the PIC$_{Total}$ (Fig. 5c).
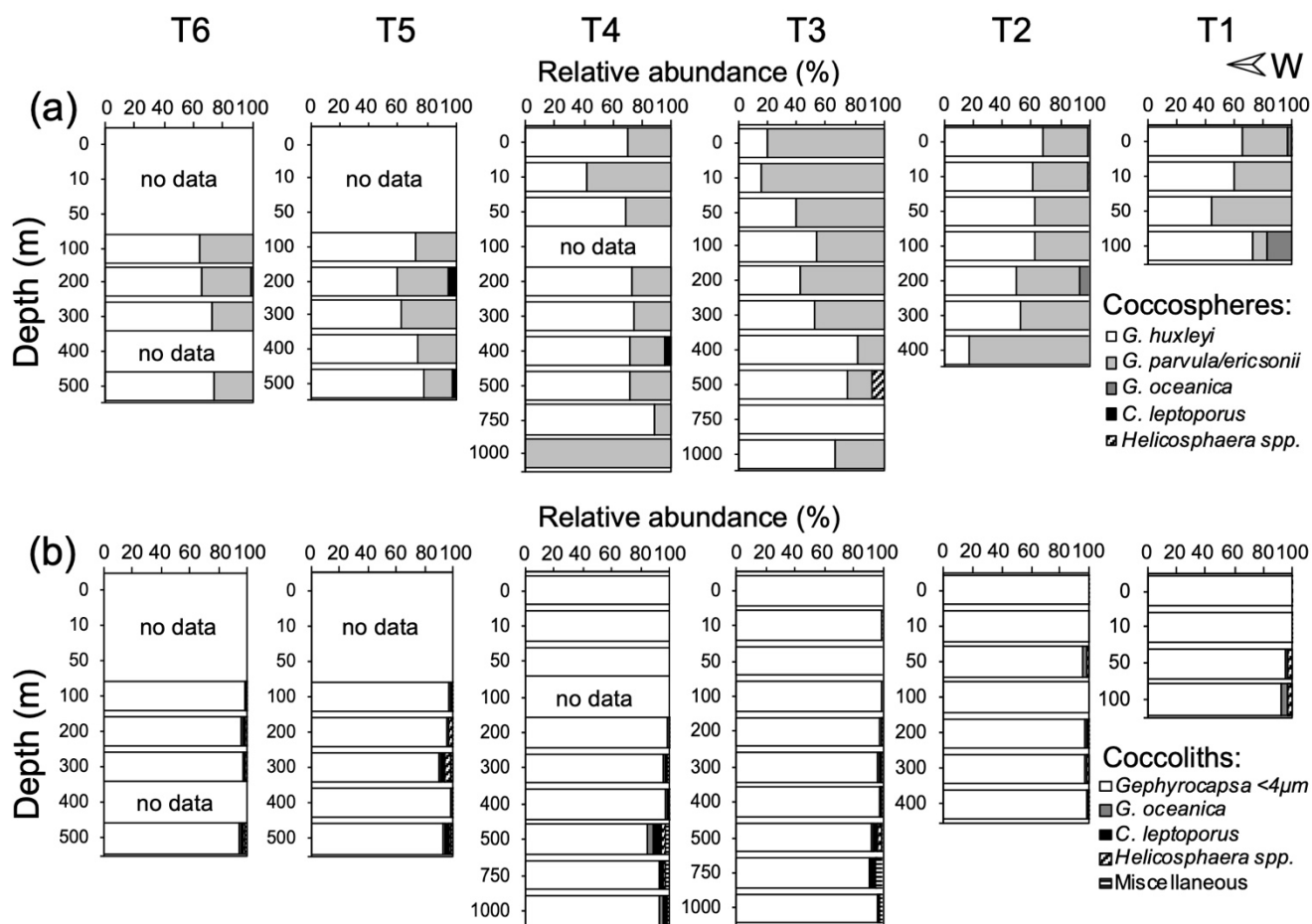
Figure 3: Coccospheres (a) and detached coccoliths (b) relative abundances in waters off Iquique (~20° S) during late-spring 2015.
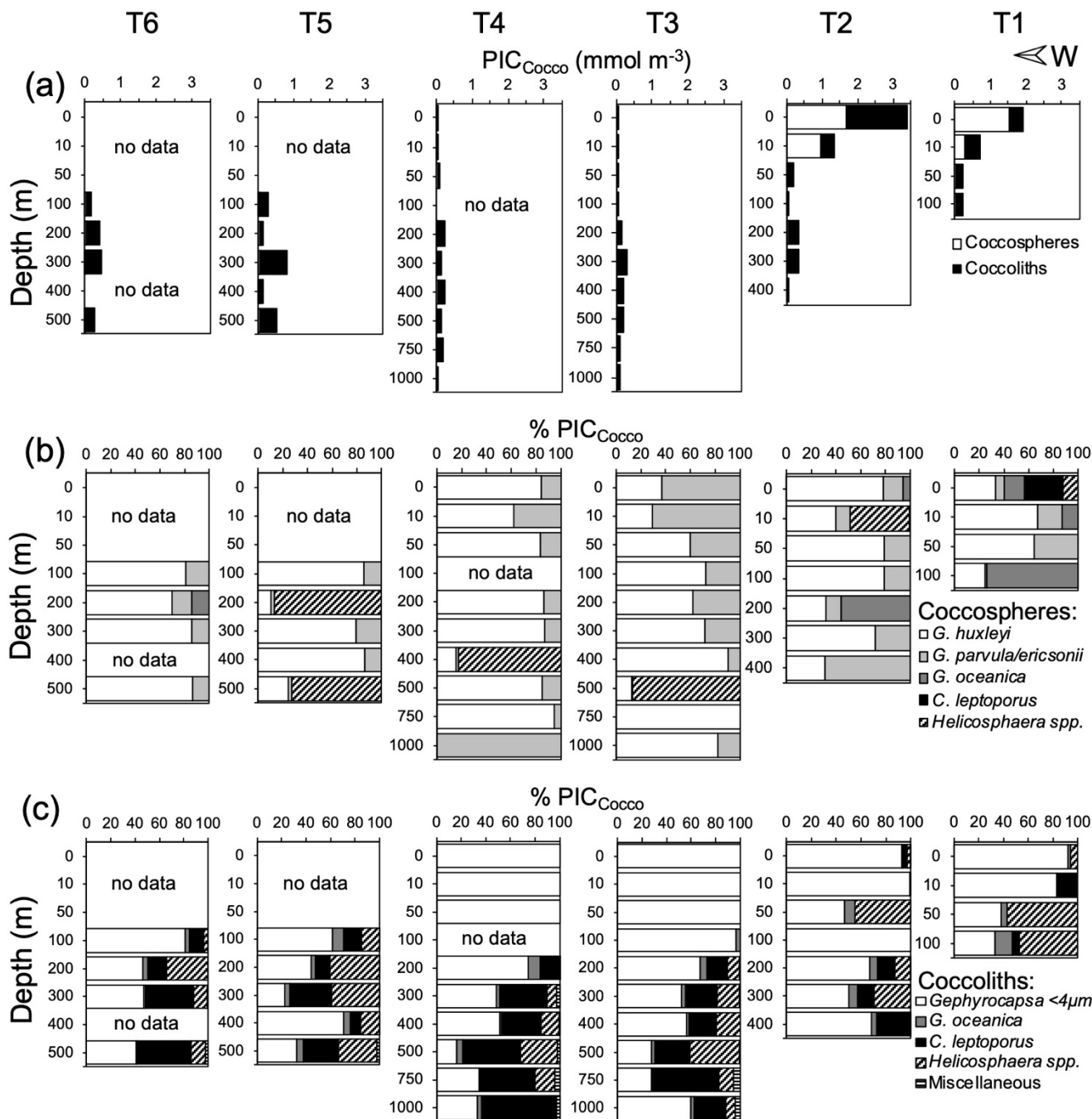
Figure 4: Estimated-PIC masses from coccospheres and detached coccoliths recorded in waters off Iquique (~ 20° S) during late-spring 2015. The contribution to PIC attributed to coccospheres and coccoliths (a), as well the taxonomic breakdown of the contribution of coccospheres (b) and detached coccoliths (c) are given.
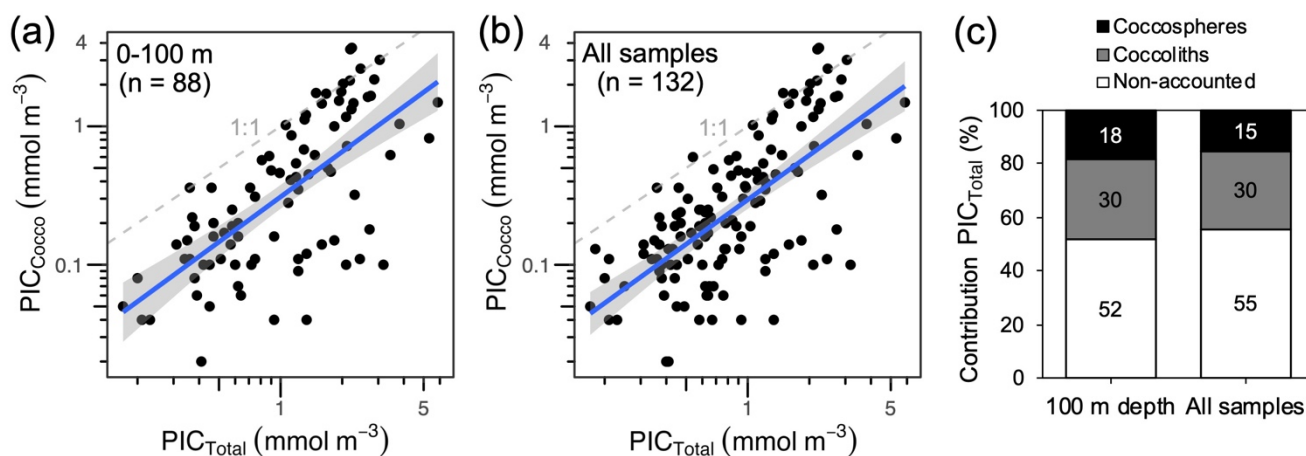
Figure 5: Linear dependence between the PIC_{Total} and PIC_{Cocco} quotas (a-b), along with the bulk proportion of PIC_{Total} accounted for by PIC_{Cocco} (c) including data from 0 to 100 m depth as all samples. PIC_{Total} and PIC_{Cocco} show a significant correlation (a): $Y = 1.082(\pm 0.126)X - 1.173(\pm 0.100)$; $R^2_{(adjusted)} = 0.45$; p-value$_{(slope, constant)} < 0.05$; n = 88 samples, as well as across all samples (b): $Y = 1.068(\pm 0.102)X - 1.220(\pm 0.077)$; $R^2_{(adjusted)} = 0.46$; p-value$_{(slope, constant)} < 0.05$; n = 132 samples. Solid blue line in (a-b) is the least squares fit, and grey areas depict 95 % confidence intervals. Dashed line in (a-b) is the 1:1 line. Note the log-log axes enable assessment of PIC_{Cocco} quota estimation performance over ~2 orders of magnitude of PIC_{Total} concentsdration. PIC = Particulate Inorganic Carbon.

3.4 Coccoliths and PIC variation across environmental conditions

Coccospheres, detached coccoliths, PIC pools, and the estimated PIC_{Cocco} quotas were marginally higher during mid-summer 2018 than in late-spring 2015 (Fig. 6). The relatively higher SST (> 21 ºC) recorded westward of the stronger upwelling band closer to the coast (Fig. 2a), may be associated with these enhanced PIC_{Cocco} quotas. A shallow Z_{eu}, averaging 36 m and ranging from 26 to 50 m across both cruises (n = 22 stations; Fig. 2c-e, k-n), was observed, below which there was a sharp decline in coccolithophores and derived PIC (Fig. 6a-c). Overall, the average PIC_{Total} and PIC_{Cocco} quotas below the Z_{eu} decreased by 50 % and 83 %, respectively (Fig. 6c-d).

On average, a notable unimodal thermal response peaking at ~18ºC was observed for both PIC_{Cocco} and PIC_{Total} within the Z_{eu} (Fig. S12a, S13a). The oxycline (~50-100 µmol kg^{-1}) and pHcline (~7.7), located near the base of the Z_{eu} (Fig. 2c, h), were associated with decreased PIC levels, particularly in PIC_{Cocco} quotas (<< 1 mmol m^{-3}; Fig. S12c and S13c). Above a pH of ~7.7 (Ω calcite > 2.0; these two variables were highly correlated), PIC_{Cocco} quotas displayed a clear unimodal relationship, peaking at pH ~7.9 (Ω calcite ~ 2.5-4.5; Fig. S12g, i), while PIC_{Total} showed a monotonic increase (Fig. S13g, i). Nutrients and pCO_2, both essential for phytoplankton growth, were consistently available below the Z_{eu} (Fig. 2f-g), with phosphate being more limiting than nitrate (Fig. S12e-f). pCO_2 levels below 800 µatm corresponded to an average increase in PIC values (Fig. S12h, S13h). Low-to-moderate Chl-a levels (< 4 mg m^{-3}) were associated with enhanced PIC_{Cocco} (> 2 mmol m^{-3}) and PIC_{Total} quotas (> 3 mmol m^{-3}), although only PIC_{Cocco} returned to background levels at higher Chl-a concentrations (Fig. S12d, S13d).
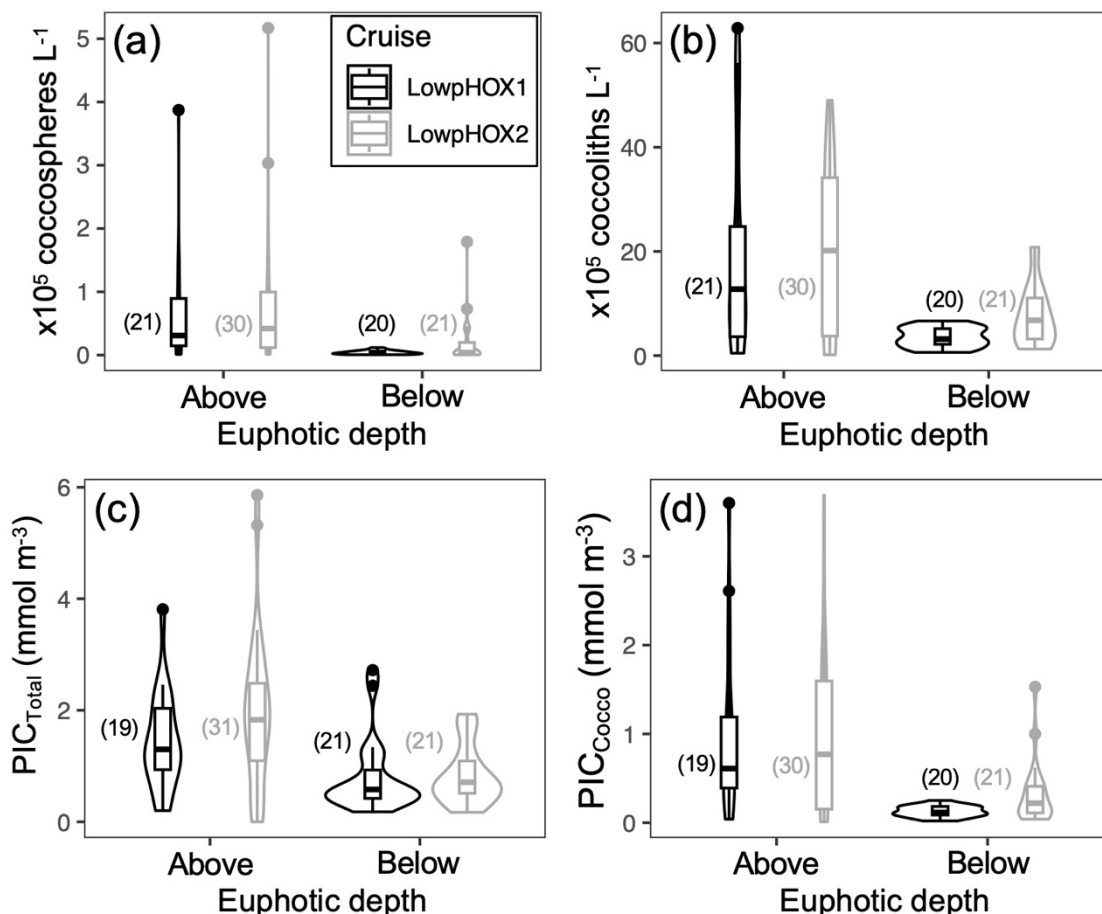
Figure 6: Violin plots comparing the variation in coccospheres (a), detached coccoliths (b), PIC$_{Total}$ (c), and PIC$_{Cocco}$ (d) above and below the euphotic depth during late-spring 2015 and mid-summer 2018. Only samples taken in the upper 100 m depth are included. The number of samples tested per category is given in parentheses.

4 Discussion

4.1 Coccolithophore species diversity and dominance off the Southeast Pacific margin

Coccospheres and detached coccoliths of *G. huxleyi* were dominant in 2018 at 20° S, as well as south of 20° S in both 2015 and 2018. This pattern is shared with other eastern boundary current systems, where *G. huxleyi* dominates numerically in waters off the Northeast Pacific (Ziveri et al., 1995; Venrick, 2012) and the Southeast Atlantic margins (Siegel et al., 2007; Henderiks et al., 2012). However, in addition to *G. huxleyi*, *G. parvula/ericsonii* were co-dominant members of the coccolithophore communities at ~20º S in 2015. The co-dominance of these three species was previously reported in winter samples from 2013 in the same zone (von Dassow et al., 2018; Díaz-Rosas et al., 2021). Likewise, "small *Reticulofenestra* complex" (presumably mostly *G. parvula*) and "small *Gephyrocapsa* complex" have been previously reported as important in

tropical and equatorial waters further offshore (Hagino and Okada, 2004), so these species are frequently important in these and neighbouring waters. To the south, co-dominance of *G. huxleyi* and *G. muellerae* has been reported previously (e.g., Díaz-Rosas et al., 2021). Thus, while the coccolithophore richness remains low in the Eastern South Pacific margin, this region exhibits a higher diversity within the genus *Gephyrocapsa* compared to other Eastern Boundary Currents (Henderiks et al.,

270   2012; Venrick, 2012). Standing stocks of larger taxa were only noticeable below the Z_{eu} (~50 m depth). It should be noted that each coccosphere or detached coccolith of *C. leptoporus* is equivalent to approximately 80 coccospheres or 45 coccoliths of *G. huxleyi* in terms of PIC. This suggests that the heavier coccoliths of these larger species may sink more efficiently (e.g., Menschel et al., 2016; Guerreiro et al., 2021).

4.2 The chemical PIC measurements as proxy of coccolithophore densities

275   How much coccolithophores contribute to PIC is an open question, as contributions from other phytoplankton, lithogenic sources (Daniels et al., 2012), and the effects of fragmentation and dissolution in the water column (e.g., Barrett et al., 2014; Subhas et al., 2022) can complicate the relation between PIC and coccolithophores, whether in remote sensing algorithms or as paleoproxy indicators. This emphasizes the value of microscopy counts, which have been found to be effective in quantifying PIC due to coccolithophores (D'Amario et al., 2018; Guerreiro et al., 2021; Ziveri et al., 2023). In this study, the

280   conversion of detached and cell-attached coccoliths to PIC_{Cocco} values showed a direct relationship with PIC_{Total} within 100 m and across all samples, with detached coccoliths contributing significantly to PIC quotas. Microscopically-countable coccoliths and coccospheres account for approximately 50 % of direct PIC measurements. In the relatively narrow shelf in north-central Chile, other potential PIC sources, such as resuspension of biogenic minerals or river discharges of lithogenic material (Daniels et al., 2012), are negligible. However, technical or methodological challenges—including the detection of smaller coccoliths,

285   collapsed coccospheres, and fragmented coccoliths, as well as variability in mass conversion factors and PIC production by other planktonic organisms—may account for the remaining PIC_{Total}. These results support the conclusion that coccolithophores are important contributors to total PIC pools in this OMZ.

4.3 Surface variation in coccolithophores and PIC quotas

Events of increased *G. huxleyi* coccospheres (> 3.0×10^5 L^{-1}), along with detached coccoliths (> 30×10^5 L^{-1}), were observed

290   in the upper waters during both late-spring 2015 and mid-summer 2018. Consequently, the PIC_{Total} and PIC_{Cocco} quotas rose to 3-5 mmol m^{-3}, representing approximately a threefold increase compared to background levels. Coccosphere and detached coccolith densities were particularly high at 20° S, with inshore station T2 in 2015 showing 12 $\times 10^6$ coccoliths L^{-1} at 2 m depth and offshore station T5 in 2018 showing 10 and 12 $\times 10^6$ coccoliths L^{-1} at 25 and 30 m depth, respectively. These densities are about an order of magnitude lower than the typical bloom abundances reported in the Southwest Atlantic (Poulton et al., 2013),

295   the North Atlantic (Holligan et al., 1993a), and the Gulf of Maine (Balch et al., 1991).

On average, higher coccolith densities, PIC_{Total}, and PIC_{Cocco} quotas were recorded during mid-summer 2018 compared to late-spring 2015, suggesting potential seasonality in PIC levels. This observation aligns qualitatively with satellite-PIC retrievals

showing PIC concentrations in February 2018 extending further offshore and southward from the inshore 20° S sampled site (see Fig. S14). Such seasonality, even though recorded in separate years, supports global satellite-PIC estimations showing

300 higher inventories off the coasts of Chile and Namibia from austral spring (October-November) peaking in summer (January-February; see Hopkins et al., 2019).

In contrast to the greater excess of detached-coccolith over coccosphere ratios observed during massive blooms (e.g., Balch et al., 1991; Holligan et al., 1993b), lower ratios (< 16) were associated with max. PIC_{Cocco} quotas (> 3 mmol m^{-3}) at station T2 in 2015 (2 m depth) and station T5 in 2018 (25 and 30 m depth). While these lower ratios might indicate younger populations

305 (Balch et al., 1991; Holligan et al., 1993b; Lessard et al., 2005), cell-attached coccoliths comprised 51-72 % of the PIC_{Cocco} quotas. This could represent the max. standing stocks and PIC quotas attainable in the Southeast Pacific margin (see Table 4 in Díaz-Rosas et al., 2021). Two factors might limit coccolithophore populations from forming massive blooms similar to those seen in the North Atlantic. First, high productivity waters are typically dominated by diatoms, which may outcompete coccolithophores (Menschel et al., 2016). Second, the low pH typical of upwelled water in this region inhibits the growth of

310 many coccolithophore strains (Sciandra et al., 2003; Bach et al., 2011; Meyer and Riebesell, 2015; Müller et al., 2015; von Dassow et al., 2018), even those isolated from the same region, which would presumably be best adapted to tolerate such conditions (von Dassow et al., 2018).

Coccolith PIC stocks varied significantly with SST, with higher PIC levels (PIC_{Cocco} and PIC_{Total}) around 18 °C during late-spring 2015 and mid-summer 2018 (Fig. S13a), suggesting a transition between nutrient-rich coastal upwelling and nutrient-

315 poor offshore waters. Moderate nutrient availability and stratification seem to promote coccolithophore growth, reflected in peak abundances and PIC quotas, particularly in 2018 following stratification due to low SST and SSS water masses (Vargas et al., 2021; Fig. 2a-b). Similar trends were observed off the Santa Barbara coast, where higher temperatures and stratification increased coccolithophore abundance and PIC quotas (Matson et al., 2019). High coccolithophore abundances also occur in upwelling regions like the equatorial Pacific (Balch and Kilpatrick, 1996) and Arabian Sea (Balch et al., 2000), and in semi-

320 oligotrophic areas such as the northern fjords, North Sea and Atlantic Ocean, under high-light conditions (Tyrrell and Merico, 2004; Zondervan, 2007). Coccolithophore blooms and PIC production are boosted after spring diatom blooms in upwelling zones, aligning with Margalef's (1978) successional model, which links their blooms to lower nutrients and turbulence than diatoms. Strong stratification with moderate nutrients favours higher PIC_{Cocco} and PIC_{Total} quotas, and indicating an inverse relationship between coccolithophores and diatoms under varying conditions (Menschel et al., 2016; Díaz-Rosas et al., 2021).

325 Environmental factors like pHcline and oxycline at the euphotic zone base may limit coccolithophore growth by impacting calcification and photorespiration. Off the Southeast Pacific, oxygen-deficient, acidic subsurface waters show pH and carbonate saturation shift (Ω calcite) to levels expected by 2100 (below 7.7 and 1.0, respectively) (Fig. 7; also see Vargas et al., 2021). The highest PIC quotas were associated with oxygenated waters, indicating phytoplankton reliance on these conditions for survival (Wong et al., 2023).

330 This study presents the first *in situ* PIC measurements from the OMZ waters off the Southeast Pacific margin, corresponding to late-spring 2015 and mid-summer of 2018. The observed PIC levels were about half those reported across the Great Calcite

Belt during winter or springtime waters off the Bay of Biscay. However, the range of PIC levels observed is consistent with ranges reported during spring off the California coast, and during summer in Patagonian shelf adjacent Atlantic waters (Table 1). Recently, enhanced coccolithophore and PIC pools were observed in February to the west in the central Pacific, with a

335 max. PIC_{Cocco} quota of ~1.3 mmol m^{-3}, representing about one-third of the PIC quotas estimated in this study (Oliver et al., 2023; refer to Table 1). More similar PIC_{Total} quotas were reported by Matson et al. (2019) off the Santa Barbara Channel, with a value of ~5.6 mmol m^{-3}. As an upper threshold of PIC_{Cocco} quotas, the most densely recorded pool of ~400 x10^6 coccoliths L^{-1} in the Gulf of Maine (Balch et al., 1991) and North Atlantic (Holligan et al., 1993a) correspond to approximately 120 mmol m^{-3} via allometric mass conversion.

340 Our dataset revealed relatively high coccolithophore PIC quotas during November and February at the border of the Southeast Pacific "PIC-data desert" (i.e., compared to the Atlantic Ocean; see Balch et al., 2018). In this context, the weekly and monthly satellite-PIC estimations, which did not exceed 1 mmol m^{-3} (average ~ 0.2-0.3 mmol m^{-3}; Fig. S14), consistently underestimated these max. PIC quotas by a factor of 3-5. Additionally, satellite-PIC retrievals overestimated the PIC_{Cocco} quotas by a factor of 2-5 across the New Zealand and Drake Passage sectors of the Southern Ocean (Saavedra-Pellitero et al, in press). It has been recently stressed that these optical PIC proxies need to be geographically adjusted (Balch and Mitchell,

345 2023). The highest PIC_{Cocco} quotas observed between 60 and 200 m depth during spring/summer in the remote Southeast Pacific (Beaufort et al., 2008; Oliver et al., 2023) likely reflect site-dependent biophysical constraints. Overall, these findings highlight the dynamic nature of coccolithophore populations and their PIC contributions, emphasizing the need for ongoing monitoring to understand their ecological roles and responses to environmental changes. Although the data are still limited,

350 and the periods sampled in this study were characterized by stratified summer water column conditions which may be conducive to coccolithophore growth (e.g., Matson et al., 2019), it is noteworthy that this zone, characterized by exceptionally low pH in sub-surface waters frequently brought to the surface by upwelling or breaking waves, does not exhibit a significant deficiency in surface layer PIC standing stocks (Fig. 8a-b).
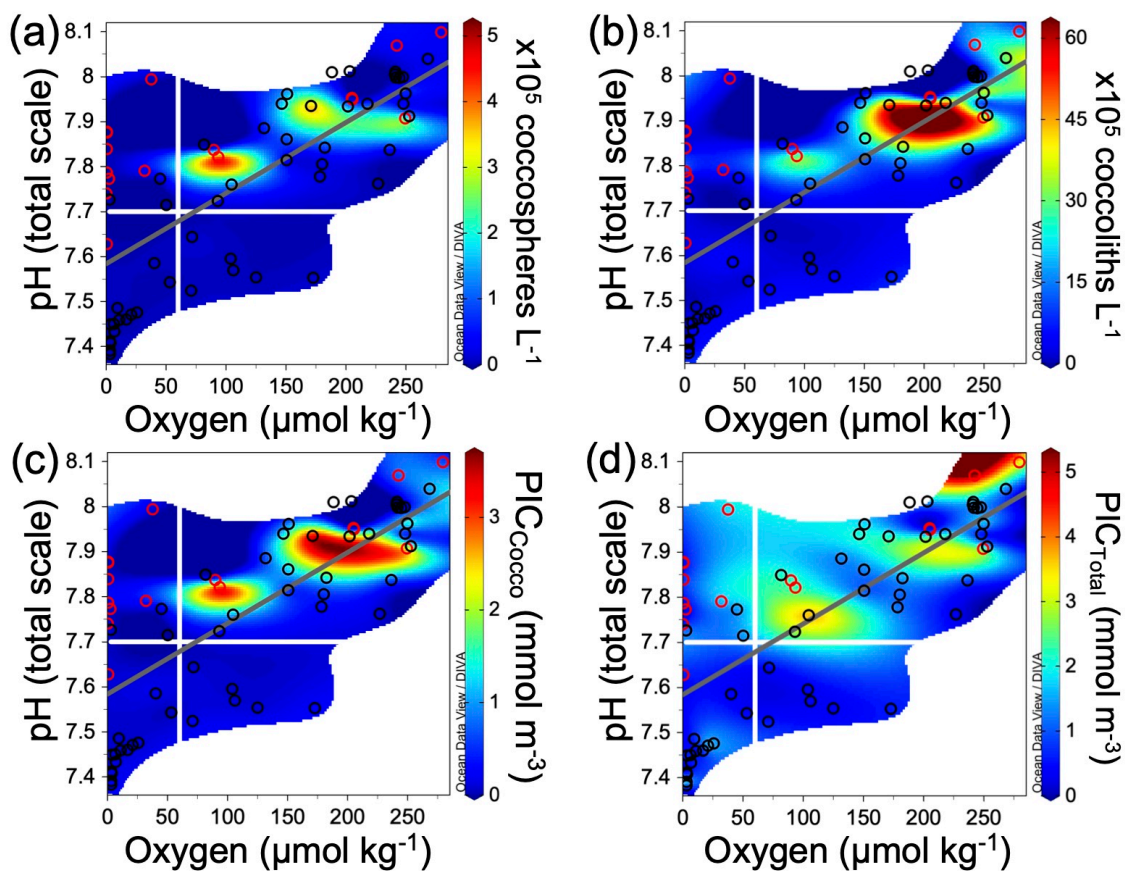
355

Figure 7. Variation in coccospheres (a), detached-coccoliths (b), PIC$_{Cocco}$ (c), and PIC$_{Total}$ pools (d) across oxygen and pH levels recorded within 100-m during late-spring 2015 (open black dots) and mid-summer 2018 (open red dots). Horizontal and vertical white lines indicate the expected pH values for 2100 and oxygen contour for the Eastern Equatorial Pacific Ocean proposed by Stramma et al. (2008), respectively. Gray line depicts the least-square model fit curve.

Table 1: Comparison of Particulate Inorganic Carbon standing stocks reported in different oceanic areas or shelf/coastal margins. 360 **The full range across all-station depths is given. AMT – Atlantic Meridional Transect; SP – Spring; AU – Autumn; WI – Winter; SU – Summer.**

Sampling domain (Cruise)	Season/Year	PIC (mmol m^{-3})	# Sts. profiles	Source
North and South Atlantic (AMT14)	AU/2004	0.001 – 0.33	27	1
Southeast Pacific (BIOSOPE)	SP/2004	0.05 – 0.35[a]	20	2
Scotia Sea/Drake Passage (JR163)	SP/2006	0.001 – 1.3	31	3
North and South Atlantic (AMT15-22)	SP, AU/2004-12	0.001 – 6.98	481	
South Atlantic/Patagonia (COPAS08)	SP/2008	0.002 – 4.31	33	
Southern Ocean/Atlantic (G. Belt-I)	SU/2011	0.002 – 9.81	31	4
Western Arctic (ICESCAPE'11)	SU/2011	< 0.001– 0.74	16	
Southern Ocean/Indian (G. Belt-II)	SU/2012	0.001 – 0.82	32	
Northeast Atlantic margin	WI, SP/2009-10	0.07 – 11.7	Upper	5
Northeast Atlantic margin (D381)	AU/2012	0.09 – 1.4	21	6
Santa Barbara channel	SP/2015	up to ~5.6	Upper	7
Southern Ocean/Pacific (RR2004)	SU/2021	up to ~1.3[b]	Upper	8
Southeast Pacific margin (LowpHOX 1)	SP/2015	0.18 – 3.81	12	This study
Southeast Pacific margin (LowpHOX 2)	SU/2018	0.08 – 5.86	10	

[a] Estimated using the "Particle Analyser" software that automatically detects and measures all birefringent particles from grabbed frames. [b] Estimated from underway "acid-labile backscattering" measurements calibrated with PIC measurements obtained with the same 365 methodology outlined above. All other studies the PIC was measured chemically with mass spectrophotometry. 1 Poulton et al. (2006); 2 Beaufort et al. (2008); 3 Holligan et al. (2010); 4 Balch et al. (2018); 5 Daniels et al. (2012); 6 Painter et al. (2016); 7 Matson et al. (2019); 8 Oliver et al. (2023).

4.4 Subsurface variation in PIC and PIC:POC ratios

Subsurface coccolithophore PIC is mostly due to detached coccoliths. While detached coccoliths of *G. huxleyi* and other small 370 *Gephyrocapsa* remain important, larger and rare species with the heaviest coccoliths, such as *C. leptoporus* and *H. carteri*, became relatively more important to PIC quotas below the Z_{eu}, as seen previously in other regions (e.g., Ziveri et al., 2007; Guerreiro et al., 2021) and even in neighbouring waters (Menschel et al., 2016).

On average, up to two-thirds of the PIC_{Cocco} quotas were present as detached coccoliths (Fig. 5c), similar to records within blooms in the North Atlantic (Fernández et al., 1993; van der Wal et al., 1995) and North Pacific (Ziveri et al., 2023). This 375 detrital material is expected to ballast POC to the deep ocean (e.g., Klaas and Archer, 2002). Additionally, a greater decrease in PIC_{Cocco} than PIC_{Total} below the Z_{eu} (Fig. 6c-d) is consistent with aggregation and fragmentation of coccoliths contributing to the non-accounted PIC_{Total}, which could sink even more POC (Briggs et al., 2020).

Previous research indicated that the transfer of POC from the euphotic zone to the deeper ocean is intensified in OMZs (Cavan et al., 2017; Engel et al., 2017). Significantly elevated PIC:POC ratios recorded within the OMZ-core (Fig. 8c; p-value < 0.05)

380 suggest that sinking particles are enriched in denser inorganic carbon (PIC), enhancing their 'ballast effect' and causing them to sink faster (Lee et al., 2009; Iversen and Ploug, 2010). This rapid descent decreases decomposition time in the upper water column, allowing more POC to reach the OMZ. These findings may indicate less POC decomposition below surface waters (e.g., between 100-1000 m; see Weber and Bianchi, 2020), as the 'ballast effect' of PIC could limit microbial degradation of POC in the mesopelagic. Ω calcite remained above 1 in the OMZ mesopelagic and the higher PIC:POC ratio in the OMZ layer

385 suggests that dissolution processes (for example in microenvironment of lower Ω calcite) are not fully offsetting the export of PIC from the surface layer. Nevertheless, these PIC:POC ratios were significantly lower compared to those in the Atlantic Ocean, Southern Ocean, and Patagonian shelf (Fig. 8).

Nevertheless, the data suggest that PIC plays a decreased role in POC export from the surface in these OMZ waters: The PIC:POC ratios were significantly lower than other diverse regions for which data are available (Fig. 8). The reasons for this are not yet clear. One possibility is that the intrusion of nutrient-rich but low pH waters into the surface further stimulates POC production from other phytoplankton (e.g., diatoms) over coccolithophores.
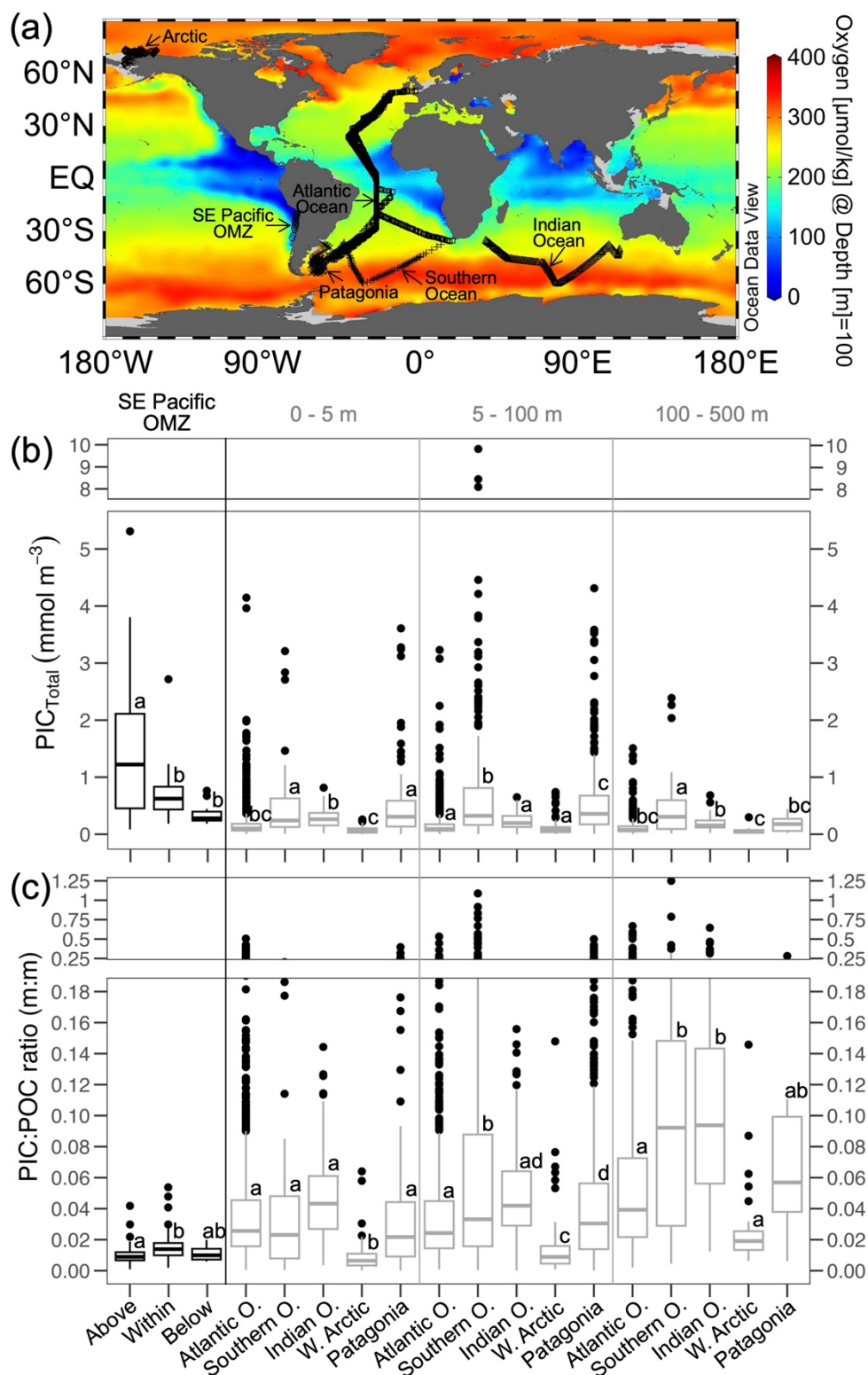
Figure 8: (a) Global map showing annual oxygen content at 100 m depth and sampling points for (b) PIC_{Total} and (c) PIC:POC ratios above, within, and below the OMZ-core during late-spring 2015 and mid-summer 2018 in the SE Pacific (this study), as well as surface (< 5 m), sub-surface (5-100 m), and below-surface waters (100-500 m) from other open ocean or coastal margin areas (data from Balch et al., 2018). Atlantic Ocean dataset comprises six cruises (AMT17-22). According to one-way ANOVAs, PIC_{Total} and PIC:POC ratios were significantly different among the SE Pacific OMZ-core, and also among the Atlantic Ocean, Southern Ocean, Indian Ocean, Western Arctic, and Patagonian Shelf sample groups ($p < 0.05$), with Tukey post-hoc multiple comparisons depicted as lowercase letters over each boxplot. Map produced by Ocean Data View (Schlitzer, 2024), with oxygen annual climatology based on the World Ocean Atlas 2018 (Boyer et al., 2018; García et al., 2018).

5 Conclusions

The examination of the coccolithophores, along with the PIC standing stocks between late-spring 2015 and mid-summer 2018 waters off the Southeast Pacific margin, yielded six conclusions:

1. Coccolithophores-PIC quotas peak within the first 30 m depth, with slightly higher PIC pools observed in summer 2018 compared to spring 2015. Spring exhibits greater variability and lower mean coccospheres and detached-coccoliths, as well as derived PIC, compared to summer.

2. *G. huxleyi*, along with *G. parvula*/*ericsonii*, co-dominate the coccosphere pools, while *G. huxleyi* is the primary contributor to detached coccoliths in the cross-shelf transect sampled at ~20º S. The majority of PIC contributed by coccolithophores is dominated by *G. huxleyi* coccoliths shed during blooms. South of 20º S, the coccospheres and detached coccoliths of *G. huxleyi* were observed as the most important contributor to biogenic calcium carbonate.

3. Both the PIC_{Total} and PIC_{Cocco} quotas decreased by 50 % and 83 % below the euphotic depth, coinciding with the oxycline and pHcline.

4. Horizontal and vertical variation in PIC_{Total} and PIC_{Cocco} quotas strongly depends on temperature, along with oxygen and pH levels.

5. PIC quotas were similar to those in other upwelling zones, and a half of max. quotas in the Atlantic Ocean and Bay of Biscay.

6. Low PIC:POC ratios, compared to other open ocean and coastal margin areas, were more pronounced within the OMZ-core, suggesting calcification plays a role in POC fluxes to deep ocean and that this role may be decreased in sub-surface OMZs compared to other zones.

Data availability.

All data generated in this study are available upon request from the corresponding author. The scanning electron micrograph image datasets are accessible at https://doi.org/10.5281/zenodo. 14048319 (Díaz-Rosas et al., 2024). The PIC measurements, as well as coccosphere and detached coccolith count data, will soon be available in the PANGAEA repository. These data are currently provided in Supplementary Tables S1-S2.

Sample availability.

Supplement.

Author contributions.

FDR (conceptualization, data curation, formal analysis, investigation, methodology, visualization, writing – original draft
425 preparation, writing – review and editing) provided key proof-of-concept ideas, led the study, conducted polarized light and
SEM microscopic analyses and taxonomic characterization of coccospheres and detached coccoliths, examined the
relationships between PIC measurements, coccolithophore pools, and environmental/biological variables, compared PIC and
PIC:POC values with existing repositories, and drafted the initial manuscript. PvD (conceptualization, funding acquisition,
validation, visualization, writing – original draft preparation, writing – review and editing) defined the research goals, led the
430 study, conducted sampling during the 2015 cruise, planned the 2018 sampling, and provided continuous insights into results
interpretation and manuscript structure. CV (funding acquisition, validation, writing – review and editing) guided the
interpretation of results and contributed to characterizing the physical and chemical environments. All co-authors provided
critical feedback and contributed to the final editing of the manuscript.

Competing interest.

435 The contact author has declared that none of the authors has any competing interests.

Acknowledgements.

We thank Dr. William Balch, Dr. Catherine Mitchell, and Dr. David Drapeau for reading and providing valuable discussion
on the manuscript.

Financial support.

440 This study was supported by the National Agency for Research and Development (ANID) of Chile through grants AIM23-
0003 and ICN12_019N for the Millennium Institute of Oceanography (IMO), as well as FONDECYT grant 1181614. Scanning
electron microscopy analysis was performed at the Centro de Investigación en Nanotecnología y Materiales Avanzados (CIEN)
of the Pontificia Universidad Católica de Chile using an SEM instrument purchased with FONDEQUIP grant EQM150101.

References

445 Bach, L. T., Riebesell, U., and Schulz, K.: Distinguishing between the effects of ocean acidification and ocean carbonation in the coccolithophore Emiliania huxleyi, Limnology and Oceanography, 56, 2040–2050, https://doi.org/10.4319/lo.2011.56.6.2040, 2011.

Balch, W. M.: Underway Data (SAS) from R/V Roger Revelle KNOX22RR in the Patagonian Shelf (SW South Atlantic) from 2008-2009 (COPAS08 project). Biological and Chemical Oceanography Data Management Office (BCO-DMO). (28 June
450 2010), 2010.

Balch, W. M.: The Ecology, Biogeochemistry, and Optical Properties of Coccolithophores, Annual Review of Marine Science, 10, 71–98, https://doi.org/10.1146/annurev- marine- 121916- 063319, 2018.

Balch, W. M. and Kilpatrick, K.: Calcification rates in the equatorial Pacific along 140°W, Deep Sea Research Part II: Topical Studies in Oceanography, 43, 971–993, https://doi.org/10.1016/0967-0645(96)00032-x, 1996.

455 Balch, W. M. and Mitchell, C.: Remote sensing algorithms for particulate inorganic carbon (PIC) and the global cycle of PIC, Earth-Science Reviews, 239, 104363, https://doi.org/10.1016/j.earscirev.2023.104363, 2023.

Balch, W. M., Holligan, P., Ackleson, S., and Voss, K.: Biological and optical properties of mesoscale coccolithophore blooms in the Gulf of Maine, Limnology and Oceanography, 36, 629–643, https://doi.org/10.4319/lo.1991.36.4.0629, 1991.

Balch, W. M., Drapeau, D. T., and Fritz, J.: Monsoonal forcing of calcification in the Arabian Sea, Deep Sea Research Part II:
460 Topical Studies in Oceanography, 47, 1301–1337, https://doi.org/10.1016/S0967-0645(99)00145-9, 2000.

Balch, W. M., Bates, N. R., Lam, P., Twining, B. S., Rosengard, S. Z., Bowler, B. C., Drapeau, D. T., Garley, R., Lubelczyk, L. C., Mitchell, C., and Rauschenberg, S.: Factors regulating the Great Calcite Belt in the Southern Ocean and its biogeochemical significance, Global Biogeochemical Cycles, 30, 1124–1144, https://doi.org/10.1002/ 2016GB005414, 2016.

Balch, W. M., Bowler, B. C., Drapeau, D. T., Lubelczyk, L. C., and Lyczsckowski, E.: Vertical Distributions of
465 Coccolithophores, PIC, POC, Biogenic Silica, and Chlorophyll a Throughout the Global Ocean, Global Biogeochemical Cycles, 32, 2–17, https://doi.org/10.1002/ 2016GB005614, 2018.

Barcelos e Ramos, J., Müller, M., and Riebesell, U.: Short-term response of the coccolithophore Emiliania huxleyi to an abrupt change in seawater carbon dioxide concentrations, Biogeosciences, 7, 177–186, https://doi.org/10.5194/bg-7-177-2010, 2010.

Barrett, P., Resing, J., Buck, N., Feely, R. A., Bullister, J., Buck, C., and Landing, W.: Calcium carbonate dissolution in the
470 upper 1000 m of the eastern North Atlantic, Global Biogeochemical Cycles, 28, 386–397, https://doi.org/10.1002/2013GB004619, 2014.

Beaufort, L., Couapel, M., Buchet, N., Claustre, H., and Goyet, C.: Calcite production by coccolithophores in the south east Pacific Ocean, Biogeosciences, 5, 1101–1117, https://doi.org/10.5194/bg-5-1101-2008, 2008.

Beaufort, L., Probert, I., de Garidel-Thoron, T., Bendif, E. M., Ruiz-Pino, D., Metzl, N., Goyet, C., Buchet, N., Coupel, P.,
475 Grelaud, M., Rost, B., Rickaby, R. E. M., and de Vargas, C.: Sensitivity of coccolithophores to carbonate chemistry and ocean acidification, Nature, 476, 80–83, https://doi.org/10.1038/nature10295, 2011.

Bendif, E., Probert, I., Díaz-Rosas, F., Thomas, D., van den Engh, G., Young, J., and von Dassow, P.: Recent reticulate evolution in the ecologically dominant lineage of coccolithophores, Frontiers in Microbiology, 7, 784, https://doi.org/10.3389/fmicb.2016.00784, 2016.

480   Bendif, E. M., Nevado, B., Wong, E., Hagino, K., Probert, I., Young, J. R., Rickaby, R. E. M., and Filatov, D.: Repeated species radiations in the recent evolution of the key marine phytoplankton lineage Gephyrocapsa, Nature Communications, 10, 4234, https://doi.org/10.1038/s41467-019-12169-7, 2019.

Boyer, T., García, H., Locarnini, R., Zweng, M., Mishonov, A., Reagan, J., Weathers, K., Baranova, O., Paver, C., Seidov, D., and Smolyar, I.: World Ocean Atlas 2018, 2018.

485   Briggs, N., Dall'Olmo, G., and Claustre, Hervé: Major role of particle fragmentation in regulating biological sequestration of CO2 by the oceans, Science, 367, 791–793, https://doi.org/10.1126/science.aay1790, 2020.

Brown, C. W. and Yoder, J. A.: Coccolithophorid blooms in the global ocean, Journal of Geophysical Research, 99, 7467–7482, https://doi.org/10.1029/93JC02156, 1994.

Cai, W.-J.: Estuarine and Coastal Ocean Carbon Paradox: CO2 Sinks or Sites of Terrestrial Carbon Incineration?, Annual
490   Review of Marine Science, 3, 123–145, https://doi.org/10.1146/annurev-marine-120709-142723, 2011.

Cavan, E. L., Trimmer, M., Shelley, F., and Sanders, R.: Remineralization of particulate organic carbon in an ocean oxygen minimum zone, Nature Communications, 8, 14847, https://doi.org/10.1038/ncomms14847, 2017.

Claxton, L., McClelland, H., Hermoso, M., and Rickaby, R. E. M.: Eocene emergence of highly calcifying coccolithophores despite declining atmospheric CO2, Nature Geoscience, 15, 826–831, https://doi.org/10.1038/s41561-022-01006-0, 2022.

495   D'Amario, B., Ziveri, P., Grelaud, M., and Oviedo, A.: Emiliania huxleyi coccolith calcite mass modulation by morphological changes and ecology in the Mediterranean Sea, PLoS ONE, 13, e0201161, https://doi.org/10.1371/journal. pone.0201161, 2018.

Daniels, C. J., Tyrrell, T., Poulton, A. J., and Pettit, L.: The influence of lithogenic material on particulate inorganic carbon measurements of coccolithophores in the Bay of Biscay, Limnology and Oceanography, 57, 145–153,
500   https://doi.org/10.4319/lo.2012.57.1.0145, 2012.

von Dassow, P.: Voltage-gated proton channels explain coccolithophore sensitivity to ocean acidification, Proceedings of the National Academy of Sciences, 119, e2206426119, https://doi.org/10.1073/pnas.2206426119, 2022.

von Dassow, P., Díaz-Rosas, F., Bendif, E. M., Gaitán-Espitia, J.-D., Mella-Flores, D., Rokitta, S., John, U., and Torres, R.: Over-calcified forms of the coccolithophore Emiliania huxleyi in high-CO2 waters are not preadapted to ocean acidification,
505   Biogeosciences, 15, 1515–1534, https://doi.org/10.5194/bg-15-1515-2018, 2018.

Díaz-Rosas, F., Alves-de-Souza, C., Alarcón, E., Menschel, E., González, H. E., Torres, R., and von Dassow, P.: Abundances and morphotypes of the coccolithophore Emiliania huxleyi in southern Patagonia compared to neighbouring oceans and Northern Hemisphere fjords, Biogeosciences, 18, 5465–5489, https://doi.org/10.5194/bg-18-5465-2021, 2021.

Díaz-Rosas, F., Vargas, C. A., and von Dassow, P.: Scanning Electron Microscopy Datasets – Coccospheres and detached
510   coccoliths in waters off the Southeast Pacific margin, https://doi.org/10.5281/zenodo.14048319, 2024.

Engel, A., Wagner, H., Le Moigne, F., and Wilson, S.: Particle export fluxes to the oxygen minimum zone of the eastern tropical North Atlantic, Biogeosciences, 14, 1825–1838, https://doi.org/10.5194/bg-14-1825-2017, 2017.

Fernández, E., Boyd, P. W., Holligan, P., and Harbour, D. S.: Production of organic and inorganic carbon within a large-scale coccolithophore bloom in the northeast Atlantic Ocean, Marine Ecology Progress Series, 97, 271–285,
515   https://doi.org/10.3354/meps097271, 1993.

Frada, M., Young, J., Cachão, M., Lino, S., Martins, A., Narciso, Á., Probert, I., and De Vargas, C.: A guide to extant coccolithophores (Calcihaptophycidae, Haptophyta) using light microscopy, Journal of Nannoplankton Research, 31, 58–112, https://doi.org/10.58998/jnr2094, 2010.

García, H., Weathers, K., Paver, C., Smolyar, I., Boyer, T., Locarnini, R., Zweng, M., Mishonov, A., Baranova, O., Seidov, D., and Reagan, J.: World Ocean Data 2018, Volume 3: Dissolved Oxygen, Apparent Oxygen Utilization, and Oxygen Saturation, 2018.

GEBCO: The GEBCO_2023 Grid - a continuous terrain model of the global oceans and land, https://doi.org/10.5285/f98b053b-0cbc-6c23-e053-6c86abc0af7b, 2023.

Guerreiro, C. V., Baumann, K.-H., Brummer, G. A., Valente, A., Fischer, G., Ziveri, P., Brotas, V., and Stuut, J. W.: Carbonate fluxes by coccolithophore species between NW Africa and the Caribbean: Implications for the biological carbon pump, Limnology and Oceanography, 66, 3190–3208, https://doi.org/10.1002/lno.11872, 2021.

Hagino, K. and Okada, H.: Floral Response of Coccolithophores to Progressive Oligotrophication in the South Equatorial Current, Pacific Ocean, in: Global Environmental Change in the Ocean and on Land, TERRAPUB, Japan, 121–132, 2004.

Henderiks, J., Winter, A., Elbrächter, M., Feistel, R., van der Plas, A., Nausch, G., and Barlow, R.: Environmental controls on Emiliania huxleyi morphotypes in the Benguela coastal upwelling system (SE Atlantic), Marine Ecology Progress Series, 448, 51–66, https://doi.org/10.3354/meps09535, 2012.

Hofmann, M. and Schellnhuber, H.-J.: Oceanic acidification affects marine carbon pump and triggers extended marine oxygen holes, Proceedings of the National Academy of Sciences, 106, 3017–3022, https://doi.org/10.1073/pnas.0813384106, 2009.

Holligan, P., Charalampopoulou, A., and Hutson, R.: Seasonal distributions of the coccolithophore, Emiliania huxleyi, and of particulate inorganic carbon in surface waters of the Scotia Sea, Journal of Marine Systems, 82, 195–205, https://doi.org/10.1016/j.jmarsys.2010.05.007, 2010.

Holligan, P., Fernández, E., Aiken, J., Balch, W., Boyd, P. W., Burkill, P., Finch, M., Groom, S., Malin, G., Muller, K., Purdie, D., Robinson, C., Trees, Ch., Turner, S., and van der Wal, P.: A biocheochemical study of the coccolithophore, Emiliania huxleyi, in the North Atlantic, Global Biogeochemical Cycles, 7, 879–900, https://doi.org/10.1029/93GB01731, 1993a.

Holligan, P., Groom, S., and Harbour, D. S.: What controls the distribution of the coccolithophore, Emiliania huxleyi, in the North Sea?, Fisheries Oceanography, 2, 175–183, https://doi.org/10.1111/j.1365-2419.1993.tb00133.x, 1993b.

Hopkins, J., Henson, S. A., Poulton, A. J., and Balch, W. M.: Regional Characteristics of the Temporal Variability in the Global Particulate Inorganic Carbon Inventory, Global Biogeochemical Cycles, 33, 1328–1338, https://doi.org/10.1029/2019GB006300, 2019.

Iversen, M. H. and Ploug, H.: Ballast minerals and the sinking carbon flux in the ocean: carbon-specific respiration rates and sinking velocity of marine snow aggregates, Biogeosciences, 7, 2613–2624, https://doi.org/10.5194/bg-7-2613-2010, 2010.

Klaas, C. and Archer, D.: Association of sinking organic matter with various types of mineral ballast in the deep sea: Implications for the rain ratio, Global Biogeochemical Cycles, 16, 1116, https://doi.org/10.1029/2001GB001765, 2002.

Kottmeier, D. M., Chrachri, A., Langer, G., Helliwell, K. E., Wheeler, G. L., and Brownlee, C.: Reduced H+ channel activity disrupts pH homeostasis and calcification in coccolithophores at low ocean pH, Proceedings of the National Academy of Sciences, 119, e2118009119, https://doi.org/10.1073/pnas.2118009119, 2022.

Lee, C., Peterson, M., Wakeham, S., Armstrong, R., Cochran, K., Miquel, J. C., Fowler, S., Hirschberg, D., Beck, A., and Xue, J.: Particulate organic matter and ballast fluxes measured using time-series and settling velocity sediment traps in the northwestern Mediterranean Sea, Deep Sea Research Part II: Topical Studies in Oceanography, 56, 1420–1436, https://doi.org/10.1016/j.dsr2.2008.11.029, 2009.

Lessard, E., Merico, A., and Tyrrell, T.: Nitrate:phosphate ratios and Emiliania huxleyi blooms, Limnology and Oceanography, 50, 1020–1024, https://doi.org/10.4319/lo.2005.50.3.1020, 2005.

Margalef, R.: Life-forms of phytoplankton as survival alternatives in an unstable environment, Oceanologica Acta, 1, 493–509, https://doi.org/10.4236/jmp.2019.1013103, 1978.

Matson, P., Washburn, L., Fields, E., Gotschalk, C., Ladd, T., Siegel, D., Welch, Z., and Iglesias-Rodriguez, M. D.: Formation, development, and propagation of a rare coastal coccolithophore bloom, Journal of Geophysical Research: Oceans, 124, 3298–3316, https://doi.org/10.1029/ 2019JC015072, 2019.

Menschel, E., González, H. E., and Giesecke, R.: Coastal-oceanic distribution gradient of coccolithophores and their role in the carbonate flux of the upwelling system off Concepción, Chile (36°S), Journal of Plankton Research, 38, 798–817, https://doi.org/10.1093/plankt/fbw037, 2016.

Meyer, J. and Riebesell, U.: Reviews and Syntheses: Responses of coccolithophores to ocean acidification: a meta-analysis, Biogeosciences, 12, 1671–1682, https://doi.org/10.5194/bg-12-1671-2015, 2015.

Monteiro, F. M., Bach, L. T., Brownlee, C., Bown, P., Rickaby, R. E. M., Poulton, A. J., Tyrrell, T., Beaufort, L., Dutkiewicz, S., Gibbs, S., Gutowska, M. A., Lee, R., Riebesell, U., Young, J. R., and Ridgwell, A.: Why marine phytoplankton calcify, Science Advances, e1501822, https://doi.org/10.1126/sciadv.1501822, 2016.

Morel, A.: Optical modeling of the upper ocean in relation to its biogenous matter content (case I waters), Journal of Geophysical Research, 93, 749–768, https://doi.org/10.1029/JC093iC09p10749, 1988.

Morel, A., Huot, Y., Gentili, B., Werdell, J., Hooker, S., and Franz, B.: Examining the consistency of products derived from various ocean color sensors in open ocean (Case 1) waters in the perspective of a multi-sensor approach, Remote Sensing of Environment, 111, 69–88, https://doi.org/10.1016/j.rse.2007.03.012, 2007.

Müller, M., Trull, T. W., and Hallegraeff, G.: Differing responses of three Southern Ocean Emiliania huxleyi ecotypes to changing seawater carbonate chemistry, Marine Ecology Progress Series, 531, 81–90, https://doi.org/10.3354/meps11309, 2015.

Oliver, H., McGillicuddy, D., Krumhardt, K., Long, M., Bates, N. R., Bowler, B., Drapeau, D., and Balch, W. M.: Environmental Drivers of Coccolithophore Growth in the Pacific Sector of the Southern Ocean, Global Biogeochemical Cycles, 37, e2023GB007751, https://doi.org/10.1029/2023GB007751, 2023.

Painter, S. C., Finlay, M., Hemsley, V., and Martin, A.: Seasonality, phytoplankton succession and the biogeochemical impacts of an autumn storm in the northeast Atlantic Ocean, Progress in Oceanography, 142, 72–104, https://doi.org/10.1016/j.pocean.2016.02.001, 2016.

Poulton, A. J., Sanders, R., Holligan, P., Stinchcombe, M., Adey, T., Brown, L., and Chamberlain, K.: Phytoplankton mineralization in the tropical and subtropical Atlantic Ocean, Global Biogeochemical Cycles, 20, GB4002, https://doi.org/10.1029/2006GB002712, 2006.

Poulton, A. J., Painter, S. C., Young, J. R., Bates, N. R., Bowler, B. C., Drapeau, D., Lyczsckowski, E., and Balch, W. M.: The 2008 Emiliania huxleyi bloom along the Patagonian Shelf: Ecology, biogeochemistry, and cellular calcification, Global
590 Biogeochemical Cycles, 27, 1023–1033, https://doi.org/10.1002/2013GB004641, 2013.

Ridgwell, A. and Zeebe, R.: The role of the global carbonate cycle in the regulation and evolution of the Earth system, Earth and Planetary Science Letters, 234, 299–315, https://doi.org/10.1016/j.epsl.2005.03.006, 2005.

Riebesell, U., Zondervan, I., Rost, B., Tortell, P., Zeebe, R., and Morel, F.: Reduced calcification of marine plankton in response to increased atmospheric CO2, Nature, 407, 364–367, https://doi.org/10.1038/35030078, 2000.

595 Schlitzer, R.: Ocean Data View, 2024.

Schmidtko, S., Stramma, L., and Visbeck, M.: Decline in global oceanic oxygen content during the past five decades, Nature, 542, 335–339, https://doi.org/10.1038/nature21399, 2017.

Sciandra, A., Harlay, J., Lefèvre, D., Lemée, R., Rimmelin, P., Denis, M., and Gattuso, J.-P.: Response of coccolithophorid Emiliania huxleyi to elevated partial pressure of CO2 under nitrogen limitation, Marine Ecology Progress Series, 261, 111–
600 122, https://doi.org/10.3354/meps261111, 2003.

Siegel, H., Ohde, T., Gerth, M., Lavik, G., and Leipe, T.: Identification of coccolithophore blooms in the SE Atlantic Ocean off Namibia by satellites and in-situ methods, Continental Shelf Research, 27, 258–274, https://doi.org/10.1016/j.csr.2006.10.003, 2007.

Stramma, L., Johnson, G., Sprintall, J., and Mohrholz, V.: Expanding oxygen-minimum zones in the tropical oceans, Science,
605 320, 655–658, https://doi.org/10.1126/science.1153847, 2008.

Subhas, A., Dong, S., Naviaux, J., Rollins, N., and Adkins, J.: Shallow Calcium Carbonate Cycling in the North Pacific Ocean, Global Biogeochemical Cycles, 36, e2022GB007388, https://doi.org/10.1029/2022GB007388, 2022.

Taylor, A. R. and Brownlee, C.: Calcification, in: The Physiology of Microalgae. Development in Applied Phycology, vol. 6, Springer, Cham, 2016.

610 Torres, R., Turner, D., Rutllant, J. A., Sobarzo, M., Antezana, T., and González, H. E.: CO2 outgassing off central Chile (31–30°S) and northern Chile (24–23°S) during austral summer 1997: the effect of wind intensity on the upwelling and ventilation of CO2-rich waters, Deep Sea Research Part I: Oceanographic Research Papers, 49, 1413–1429, https://doi.org/10.1016/S0967-0637(02)00034-1, 2002.

Torres, R., Pantoja, S., Harada, N., González, H. E., Daneri, G., Frangopulos, M., Rutllant, J. A., Duarte, C. M., Rúiz-Halpern,
615 S., Mayol, E., and Fukasawa, M.: Air-sea CO 2 fluxes along the coast of Chile: From CO 2 outgassingin central northern upwelling waters to CO 2 uptake in southernPatagonian fjords, Journal of Geophysical Research: Oceans, 116, C09006, https://doi.org/10.1029/2010JC006344, 2011.

Tyrrell, T. and Merico, A.: Emiliania huxleyi: bloom observations and the conditions that induce them, in: Coccolithophores, Springer Berlin Heidelberg, 2004.

620 Vargas, C., Cantarero, S., Sepúlveda, J., Galán, A., De Pol-Holz, R., Walker, B., Schneider, W., Farías, L., Cornejo, M., Walker, J., Xu, X., and Salisbury, J.: A source of isotopically light organic carbon in a low-pH anoxic marine zone, Nature Communications, 12, 1604, https://doi.org/10.1038/s41467-021-21871-4, 2021.

Vargas, C. A., Lagos, N. A., Lardies, M. A., Duarte, C., Manriquez, P. H., Aguilera, V. M., Broitman, B., Widdicombe, S., and Dupont, S.: Species-specific responses to ocean acidification should account for local adaptation and adaptive plasticity, Nature Ecology & Evolution, 1, 0084, https://doi.org/10.1038/s41559-017-0084, 2017.

Vargas, C. A., Alarcón, G., Navarro, E., and Cornejo-D'Ottone, M.: Discrete, profile measurement of dissolved inorganic carbon (DIC), total alkalinity, partial pressure of CO2, pH on total scale, water temperature, salinity, dissolved oxygen concentration and other variables obtained during the R/V Cabo de Hornos cruise Lowphox-I (ESPOCODE 20HZ20151205) in the South Pacific Ocean from 2015-12-05 to 2015-12-09 (NCEI Accession 0281723), https://doi.org/10.25921/1tgf-v522, 2023a.

Vargas, C. A., Alarcón, G., Navarro, E., and Cornejo-D'Ottone, M.: Discrete, profile measurement of dissolved inorganic carbon (DIC), total alkalinity, partial pressure of CO2, pH on total scale, water temperature, salinity, dissolved oxygen concentration and other variables obtained during the R/V Cabo de Hornos cruise Lowphox-I (ESPOCODE 20HZ20151227) in the South Pacific Ocean from 2015-11-27 to 2015-11-28 (NCEI Accession 0281749), https://doi.org/10.25921/0dg3-8e14, 2023b.

Vargas, C. A., Alarcón, G., Navarro, E., and Cornejo-D'Ottone, M.: Discrete, profile measurement of dissolved inorganic carbon (DIC), total alkalinity, partial pressure of CO2, pH on total scale, water temperature, salinity, dissolved oxygen concentration and other variables obtained during the R/V Cabo de Hornos cruise Lowphox-II (ESPOCODE 20HZ20180203) in the South Pacific Ocean from 2018-02-03 to 2018-02-06 (NCEI Accession 0281750), https://doi.org/10.25921/6202-vf47, 2023c.

Venrick, E.: Phytoplankton in the California Current system off southern California: Changes in a changing environment, Progress in Oceanography, 104, 46–58, https://doi.org/10.1016/j.pocean.2012.05.005, 2012.

van der Wal, P., Kempers, R., and Veldhuis, M.: Production and downward flux of organic matter and calcite in a North Sea bloom of the coccolithophore Emiliania huxleyi, Marine Ecology Progress Series, 126, 247–265, https://doi.org/10.3354/meps126247, 1995.

Weber, T. and Bianchi, D.: Efficient particle tranfer to depth in Oxygen Minimum Zones of the Pacific and Indian oceans, Frontiers in Earth Science, 8, 1–11, https://doi.org/10.3389/feart.2020.00376, 2020.

Werdell, J., Bailey, S., Fargion, G., Pietras, C., Knobelspiesse, K., Feldman, G., and McClain, C.: Unique Data Repository Facilitates Ocean Color Satellite Validation, EOS, 84, 377–392, https://doi.org/10.1029/2003EO380001, 2003.

Wong, J., Raven, J., Aldunate, M., Silva, S., Gaitan-Espitia, J., Vargas, C., Ulloa, O., and von Dassow, P.: Do phytoplankton require oxygen to survive? A hypothesis and model synthesis from oxygen minimum zones, Limnology and Oceanography, 68, 1417–1437, https://doi.org/10.1002/lno.12367, 2023.

Yang, T.-N. and Wei, K.-Y.: HOW MANY COCCOLITHS ARE THERE IN A COCCOSPHERE OF THE EXTANT COCCOLITHOPHORIDS? A COMPILATION, Journal of Nannoplankton Research, 25, 7–15, https://doi.org/10.58998/jnr2275, 2003.

Young, J., Geisen, M., Cros, L., Kleijne, A., Sprengel, C., Probert, I., and Østergaard, J.: A guide to extant coccolithophore taxonomy, Journal of Nannoplankton Research Special Issue, 1, 1–125, https://doi.org/10.58998/jnr2297, 2003.

Young, J. R. and Ziveri, P.: Calculation of coccolith volume and its use in calibration of carbonate flux estimates, Deep Sea Research Part II: Topical Studies in Oceanography, 47, 1679–1700, https://doi.org/10.1016/S0967-0645(00)00003-5, 2000.

660   Zhang, H., Wang, K., Fan, G., Li, Z., Yu, Z., Jiang, J., Lian, T., and Feng, G.: Feedbacks of CaCO3 dissolution effect on ocean carbon sink and seawater acidification: a model study, Environmental Research Communications, 5, 021004, https://doi.org/10.1088/2515-7620/aca9ac, 2023.

Ziveri, P., Thunell, R., and Rio, D.: Seasonal changes in coccolithophore densities in the Southern California Bight during 1991-1992, Deep Sea Research Part I: Oceanographic Research Papers, 42, 1881–1903, https://doi.org/10.1016/0967-
665   0637(95)00089-5, 1995.

Ziveri, P., Bernardi, B., Baumann, K.-H., Stoll, H., and Mortyn, G.: Sinking of coccolith carbonate and potential contribution to organic carbon ballasting in the deep ocean, Deep Sea Research Part II: Topical Studies in Oceanography, 54, 659–675, https://doi.org/10.1016/j.dsr2.2007.01.006, 2007.

Ziveri, P., Gray, W., Anglada-Ortiz, G., Manno, C., Grelaud, M., Incarbona, A., Buchanan, J., Subhas, A., Pallacks, S., White,
670   A., Adkins, J., and Berelson, W.: Pelagic calcium carbonate production and shallow dissolution in the North Pacific Ocean, Nature Communications, 14, 805, https://doi.org/10.1038/s41467-023-36177-w, 2023.

Zondervan, I.: The effects of light, macronutrients, trace metals and CO2 on the production of calcium carbonate and organic carbon in coccolithophores—A review, Deep Sea Research Part II: Topical Studies in Oceanography, 54, 521–537, https://doi.org/10.1016/j.dsr2.2006.12.004, 2007.

675